Frontiers in Bioscience Landmark

Front. Biosci. (Landmark Ed) **2025**; 30(10): 44633
https://doi.org/10.31083/FBL44633

Original Research

polr2i is Required for Zebrafish Early Cardiac Development

Yukun Chen[1,2,†], Qiuping Zhang[1,2,†], Xiaoyan Peng[2,3,4], Xinrui Wang[2,3,4], Hua Cao[5], Qiang Chen[1], Shuting Huang[1,*], Yuqing Lei[2,3,4,*]

[1]Department of Cardiac Surgery, Fujian Children's Hospital (Fujian Branch of Shanghai Children's Medical Center), College of Clinical Medicine for Obstetrics & Gynecology and Pediatrics, Fujian Medical University, 350011 Fuzhou, Fujian, China
[2]Medical Research Center, Fujian Maternity and Child Health Hospital, College of Clinical Medicine for Obstetrics & Gynecology and Pediatrics, Fujian Medical University, 350000 Fuzhou, Fujian, China
[3]Medical Research Center, Fujian Children's Hospital (Fujian Branch of Shanghai Children's Medical Center), College of Clinical Medicine for Obstetrics & Gynecology and Pediatrics, Fujian Medical University, 350011 Fuzhou, Fujian, China
[4]Fujian Key Laboratory of Women and Children's Critical Diseases Research, Fujian Maternity and Child Health Hospital, 350001 Fuzhou, Fujian, China
[5]Shengli Clinical Medical College of Fujian Medical University, Fujian Provincial Hospital, 350001 Fuzhou, Fujian, China
*Correspondence: hshuting2014@163.com (Shuting Huang); yuqinglei@fjmu.edu.cn (Yuqing Lei)
[†]These authors contributed equally.
Academic Editor: Natascia Tiso
Submitted: 8 July 2025 Revised: 12 September 2025 Accepted: 17 September 2025 Published: 13 October 2025

Abstract

Background: Congenital heart disease (CHD) is characterized by structural and functional anomalies of the heart and major blood vessels present at birth. It is recognized as the most common congenital defect. Epidemiological studies highlight the substantial contribution of genetic factors to CHD pathogenesis. In our previous study, RNA polymerase II subunit I (POLR2I protein) was identified as a candidate genetic contributor to CHD. However, its functional role remains largely unexplored. **Methods**: First, we performed bioinformatics analyses to evaluate the evolutionary conservation of the POLR2I protein across vertebrate species. The amino acid sequence similarity of the POLR2I protein exceeds 90% in different vertebrates, suggesting a correlation between their species. Quantitative real-time PCR (qRT-PCR) revealed significantly elevated *polr2i* gene expression during early embryonic stages and in adult zebrafish organs, including the heart, eyes, and brain. Morpholino oligonucleotide (MO)-mediated gene editing was used to downregulate the *polr2i* gene in zebrafish, and rescue experiments were performed by co-injecting capped *polr2i* gene mRNA. Transgenic zebrafish labeled with specific fluorescent protein facilitated detailed studies of cardiac and vascular development, myocardial mitochondrial quality, and embryonic asymmetry, respectively. Hemoglobin staining with o-Dianisidine assessed red blood cell accumulation. **Results**: Knocking down the *polr2i* gene through MO significantly disrupted developmental trajectories, as evidenced by reduced body size, axial curvature, enlarged yolk sacs, and elevated malformation and mortality rates. Rescue experiments confirmed the specificity of these phenotypes to *polr2i* gene loss. Affected embryos displayed elongated heart tubes with reduced overlap between chambers and significant pericardial edema, indicating severe cardiac malformations or functional impairments. Measured volume per beat, ejection fraction, and cardiac output decreased substantially. Furthermore, expression levels of critical cardiovascular markers were markedly reduced. Angiogenic processes were also disrupted, as evidenced by the reduced formation of intersegmental vessels and the caudal vein plexus. Impaired mitochondrial quality in myocardial cells was observed post-knockdown, along with notable defects in the left-right asymmetry of the heart, liver, and pancreas. **Conclusion**: Knockdown of the *polr2i* gene not only impairs cardiac structure and function but also disrupts the normal developmental asymmetry of multiple organs. These findings enhance our understanding of *polr2i* gene's role in CHD and underscore its potential as a therapeutic target.

Keywords: RNA Polymerase II; embryology; embryonic development; zebrafish; morpholinos

1. Introduction

Congenital heart disease (CHD), the most common birth defect, arises from abnormal cardiac or major vascular development during embryogenesis. It is also a leading cause of mortality in newborns and infants [1]. Although advances in medical interventions have improved acute-phase management of CHD, residual or postoperative complications—including heart failure, arrhythmias, hypertension, and coronary artery disease—persistently impair long-term outcomes and quality of life [2]. These conditions impose substantial burdens on families and society, underscoring the critical need for innovative strategies to mitigate the incidence of CHD. Extensive epidemiological evidence highlights genetic factors as primary etiological contributors to CHD, while environmental influences also exert significant effects [3,4]. Cardiac development is governed by an intricate network of transcription factors, signaling pathways, and genes that require precisely coordinated regulation. Disruptions within this network can precipitate CHD, highlighting the importance of elucidating

these molecular regulatory mechanisms [5,6]. Therefore, such understanding could revolutionize the diagnosis and management of CHD, offering new avenues for prevention and therapeutic intervention.

CHD exhibits marked phenotypic and genetic heterogeneity. Approximately 30% of cases are associated with chromosomal abnormalities or monogenic disorders, frequently co-occurring with severe systemic comorbidities [7]. Both humans and other vertebrates exhibit a distinct pattern of left-right organ asymmetry, deviations from which can lead to complex CHD with limited therapeutic options [8,9]. Thus, prenatal genetic screening aims to identify severe heart malformations early, potentially alleviating the extensive personal and societal costs. In a retrospective cohort study of ultrasound-diagnosed sporadic CHD cases, we performed whole exome sequencing (WES) combined with rare variant burden analysis to pinpoint pathogenic candidates [10]. This approach identified the RNA polymerase II subunit I (POLR2I protein, also known as RPB9 or hRPB14.5) as a candidate gene linked to a spectrum of severe cardiac anomalies in one CHD fetus. Fetal ultrasonography reported complete pulmonary venous ectopic drainage, right ventricular double outlet, pulmonary artery stenosis, right aortic arch and visceral ectopic.

RNA polymerase II serves as the principal transcription machinery in eukaryotic cells, orchestrating the synthesis of mRNA for protein encoding and certain non-coding RNAs. Recognized as the most dynamic and intricate of the eukaryotic RNA polymerases, its functional nuances and regulatory mechanisms, particularly those concerning its subunits, remain inadequately defined despite extensive study [11]. Among these subunits, *POLR2I* gene, situated on chromosome 19q13.12, is notable for its evolutionary conservation across eukaryotic species [12,13]. This subunit participates in critical cellular processes including DNA repair and transcription regulation [14,15]. Notably, although human *POLR2I* gene can functionally compensate for yeast *Rpb9* deletion—demonstrating conserved roles—the yeast ortholog is dispensable for viability, whereas its Drosophila homolog is essential [16,17].

Clinically, *POLR2I* gene variants have been associated with adult-onset cardiovascular and renal pathologies, including coronary artery disease [18] and hypertensive nephropathy [19]. Yet, its specific contributions to congenital heart disease (CHD) and cardiac development remain ambiguous. Based on the results of CHD whole exome sequencing, we have identified a plausible link between *POLR2I* gene mutations and CHD manifestations. This study used zebrafish (Danio rerio) as an *in vivo* model to investigate the role of *polr2i* gene in key stages of cardiac development. This choice is not only based on its traditional advantages such as embryo transparency, external visibility during development, and ease of genetic manipulation, but also on the high evolutionary conservation exhibited by zebrafish and humans in the molecular genetic pathways of heart development [20,21]. This study aims to elucidate the fundamental aspects of cardiac morphogenesis and may provide insights into new therapeutic targets for congenital heart disease.

2. Material and Methods

2.1 Zebrafish Care and Maintenance

All adult zebrafish were housed in a recirculating aquaculture system maintained at 26–28 °C with a 14-hour light/10-hour dark cycle to support optimal biorhythms. Wild-type (AB strain) and specific transgenic lines—*Tg(myl7:EGFP)*, *Tg(fli1a:EGFP)*, *Tg(fabp10a:dsRed)*, and *Tg(ela3l:EGFP)*—were procured from the China Zebrafish Resource Center (CZRC). The *Tg(cmlc2:MitoTimer)* line, which marks myocardial mitochondria, was developed in our lab to evaluate cardiac mitochondrial turnover. Adult zebrafish were maintained at a 1:1 male-to-female breeding ratio to ensure genetic diversity. All experiments were performed in triplicate under standardized conditions to ensure phenotypic reproducibility and consistency. All procedures were approved by the Animal Ethics Committee of AEC SFY 2025 058.

2.2 Morpholino Injection

Antisense morpholino oligonucleotides (MOs) targeting the *polr2i* gene splice site (*polr2i* gene-MO: 5′-ACTCATTTCAACTCACCATTCCTGA-3′) were custom-designed by Gene Tools LLC (Philomath, OR, USA). A total of 400 one-cell stage embryos were microinjected, with 200 embryos receiving *polr2i* gene-MO and 200 injected with a standard control MO (*control*-MO: 5′-CCTCTTACCTCAGTTACAATTTATA-3′). All procedures strictly adhered to the Zebrafish Community Guidelines [22]. To validate MO specificity and establish the minimum effective dose, we conducted a dose-response analysis using escalating *polr2i* gene-MO concentrations. Embryos were injected with *polr2i* gene-MO at increasing concentrations (0.3, 0.5, 0.6, 0.8 mM; corresponding to 2.4, 4.0, 4.8, 6.4 ng/embryo) or control-MO (3.0 ng/embryo). Cardiac malformations (e.g., pericardial edema, ventricular hypoplasia) and intersegmental vascular (ISV) defects were quantified at 72 hours post-fertilization (hpf) using established morphological scoring criteria. MOs were delivered into the yolk of one-cell stage embryos at a final working concentration of 0.6 mM (4.8 µg/µL), with 1 nL injected per embryo, yielding a total dose of 4.8 ng/embryo. Embryos were maintained at 28 °C in E3 medium (5 mM NaCl, 0.17 mM KCl, 0.33 mM $MgSO_4$, 0.33 mM $CaCl_2$), with microinjections performed using a TransferMan® 4R micromanipulator was coupled to a FemtoJet 4X microinjector (Eppendorf, Hamburg, Germany).

2.3 mRNA Rescue

The *polr2i* gene cDNA was cloned into the pCS2+ vector for mRNA synthesis using the mMESSAGE mMA-

CHINE T7 system (Ambion). Fertilized eggs were co-injected with *polr2i* gene MOs and capped *polr2i* gene mRNA (300 ng/μL) to assess rescue effects.

2.4 RNA Isolation, Reverse-Transcription, qRT-PCR and RT-PCR

To analyse the effects on gene transcription levels under neomycin exposure, we collected groups of 72 hpf larvae with 50 embryos per group FastPure Cell/Tissue Total RNA Isolation Kit V2 (Vazyme, Nanjing, China, Cat No. RC112–01) to extract the total mRNA. subsequently, total mRNA was extracted using the PrimePure Cell/Tissue Total RNA Isolation Kit V2 (Thermo Fisher Scientific, Waltham, MA, USA, Cat No.12183) with a cDNA was subsequently prepared using a PrimeScript RT kit with gDNA Eraser (Takara, Kusatsu, Japan, Cat No.RR047A).

Quantitative real-time PCR (qRT-PCR) procedures were performed by SYBR® Green Realtime PCR Master Mix (TOYOBO, Osaka, Japan, No. QPK-201, QPK-201T) via the QuantStudio 5 Real-Time PCR System (Thermo Fisher Scientific, Waltham, MA, USA, Cat. A28574) was performed. The internal reference was β-actin, which was analysed using the $2^{-\Delta\Delta CT}$ method.

RNA expression analysis was accomplished using PCR with Rapid Taq DNA Polymerase (Vazyme, Cat. P223-01) at 95 °C for 3 min, 94 °C for 30 sec, 55 °C for 30 sec, 72 °C for 1 min (35 cycles) with primer sets of zebrafish *polr2i* gene, primer sets of zebrafish β-actin used as a control; forward; 5′-AGCAGGATGCGGTTTTCTTTAT-3′, reverse; 5′-GCCATGCCAATGTTGTCGTT-3′. PCR products were separated by electrophoresis on 2% agarose gels to analyze the expression.

Primers used in qRT-PCR and RT-PCR are listed in **Supplementary Table 1**.

2.5 Cardiac Phenotype Analysis

To assess cardiac phenotypes, one-cell stage embryos of the *Tg(myl7:EGFP)* transgenic line were microinjected with *polr2i* gene-MO at a final concentration of 0.6 mM (equivalent to 4.8 ng/embryo). Embryos were harvested at 48 and 72 hpf for phenotypic analysis. Zebrafish larvae were anesthetized with 0.02% tricaine methanesulfonate (Sigma-Aldrich, St. Louis, MO, USA; Cat. E10521) and mounted on a 15-mm glass bottom cell culture dish (Nest, Wuxi City, Jiangsu Province, China; Cat.801002) in 3% methylcellulose (Sangon, Shanghai, China; Cat. A600616) and oriented laterally for imaging. Images were captured using a fluorescence microscope (ECLIPSE Ts2R-FL, Nikon, Chiyoda ku, Tokyo, Japan) for morphology observation.

Photographs were quantified using NIS-Elements D software (Nikon, Chiyoda ku, Tokyo, Japan) to determine the pericardial area and cardiac function per field of view. Heart rate was quantified by manual counting of ventricular contractions over three consecutive 15-second intervals per embryo and expressed as beats per minute (bpm). At the same time, images were extracted from these visual frequencies to measure the long (a) and short (b) axis lengths of the diastolic and systolic ventricles. And then calculate end-diastolic volume (EDV), end-systolic volume (ESV), stroke volume (SV), and cardiac output (CO) of the larvae. The common formula for EDV and ESV is: volume = $4/3\pi ab^2$. The calculation formula for SV is: SV = EDV – ESV, and the calculation formula for CO is: CO = SV × HR. The ejection fraction is (EDV-ESV)/EDV × 100%.

2.6 Zebrafish Angiogenesis Analysis

To assess vascular development, one-cell stage embryos of the *Tg(fli1a:EGFP)* transgenic line were microinjected with *polr2i* gene-MO (0.6 mM, equivalent to 4.8 ng/embryo). Embryos were harvested at 72 hpf and processed for analysis. Zebrafish were oriented on lateral side (anterior, left; posterior, right; dorsal, top), and mounted with 4% methylcellulose in a slide for observation by fluorescence microscopy. The morphology of the caudal vein plexus and the number of intersegmental vessels that connect the dorsal aorta to the dorsal longitudinal anastomotic vessels were analysed. Use ImageJ software (v1.53c, NIH, Bethesda, MD, USA) to analyze and measure the endpoints, number of vascular segments, and total skeleton length which can approximately represent the total length of blood vessels in the captured images.

2.7 o-Dianisidine Staining

For o-Dianisidine staining, the embryos were collected and fixed at room temperature for 4 h using 4% PFA. Following three 10-minute washes with phosphate-buffered saline containing 0.1% Tween-20 (PBST), embryos were incubated in o-dianisidine staining solution (40% ethanol, 0.65% H_2O_2, 10 mM sodium acetate, 0.6 mg/mL o-dianisidine; Sigma-Aldrich) under light-protected conditions for 30 minutes, then washed thrice with PBST. Embryos were subsequently treated with a depigmentation solution (1% KOH, 3% H_2O_2) for 2 minutes to reduce background pigmentation. Stained embryos were washed with PBST three times and stored in 80% glycerol (v/v) for imaging using a microscope (SMZ745T, Nikon).

2.8 Image Acquisition

Embryos and larvae were imaged with Nikon TS2R inverted fluorescence microscope and subsequently photographed with digital cameras. Quantitative image analyses processed using image based morphometric analysis (NIS-Elements D) with standardized thresholding parameters for all samples. Positive signals were defined by particle number using ImageJ. 10 animals for each group were quantified, and the total signal per animal was averaged.

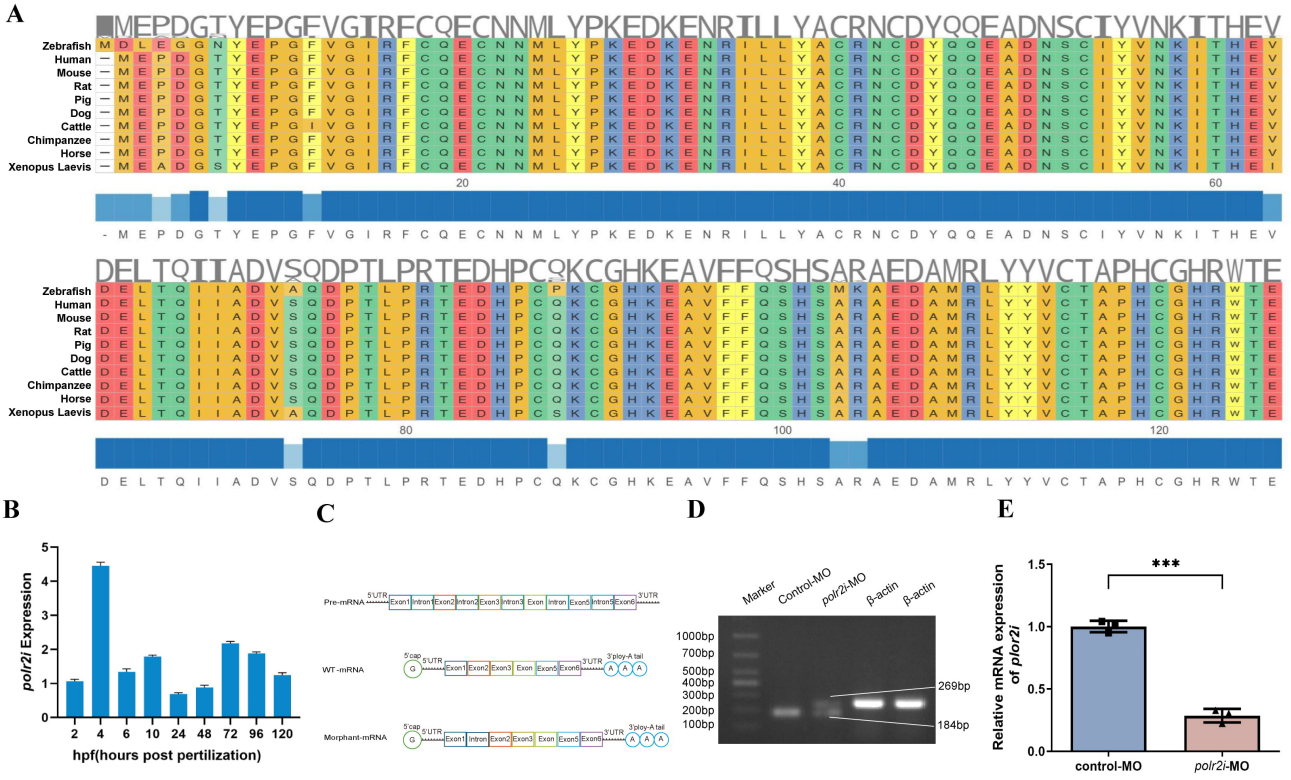

Fig. 1. POLR2I protein is evolutionarily conserved and developmentally expressed. (A) A sequence alignment of zebrafish, human, mouse, rat, pig, dog, cattle, chimpanzee, horse, and xenopus laevis POLR2I proteins by Hiplot. (B) Quantitative real-time PCR (qRT-PCR) for ten embryo development stages (2 hpf, 4 hpf, 6 hpf, 10 hpf, 12 hpf, 24 hpf, 48 hpf, 72 hpf, 96 hpf, and 120 hpf) demonstrates different expression patterns of *polr2i* gene during embryonic development (n = 50, N = 3). (C,D) Schematic representation of precursor RNA, wild-type RNA, and *polr2i* gene morphant RNA, with RT-PCR results showing that splicing regulation at the MO-targeted e1i1 junction produces an intron retention effect. (E) qRT-PCR conformation that *polr2i* gene expression is significantly decreased in *polr2i* gene-MO embryos (n = 50, N = 3). Square: control group; Triangle: experimental group. ***, $p < 0.001$. POLR2I proteins, RNA polymerase II subunit I; MO, morpholino oligonucleotides.

2.9 Statistical Analysis

All experiments included three independent biological replicates, with triplicate technical measurements per biological replicate. Data are presented as mean ± SD, as specified in figure legends. Statistical analyses were conducted using unpaired two-tailed Student's *t*-tests or one-way ANOVA with Tukey's post hoc test, as dictated by experimental design. Figure legends indicate the number of biological replicates (n) analyzed per experimental group. A value of p was considered statistically significant (*, $p < 0.05$, **, $p < 0.01$, ***, $p < 0.001$).

2.10 Euthanasia Method

After the experiment, zebrafish fry were euthanized in a buffered MS-222 solution (500 mg/L, pH ~7.0). Ensure that the fish fry are soaked in the solution for at least 30 minutes until their heartbeat completely stops, and then soak for an additional period of time to confirm death. This procedure follows the standards of the American Veterinary Medical Association (AVMA) Euthanasia Guidelines, and the MS-222 is also the most commonly used anesthetic in zebrafish research, which inhibits nerve impulse conduction by blocking neural sodium ion channels. The soaking method is usually used for administration, which can induce a rapid and reversible anesthesia state. When used, Tris or sodium bicarbonate should be buffered to neutral pH to avoid acidosis and ensure animal welfare [23].

2.11 Method Declaration

All methods in this experiment were performed in accordance with relevant guidelines and regulations.

3. Results

3.1 POLR2I Protein is Evolutionarily Conserved and is Expressed During Development

Bioinformatics analyses showed that POLR2I protein was correlated across vertebrate species (Fig. 1A). Expression patterns of the *polr2i* gene varied across different embryonic development stages of zebrafish, depicted in Fig. 1B. These findings underscore POLR2I protein's conservation among vertebrates and validate the use of the zebrafish model to investigate the implications of *polr2i*

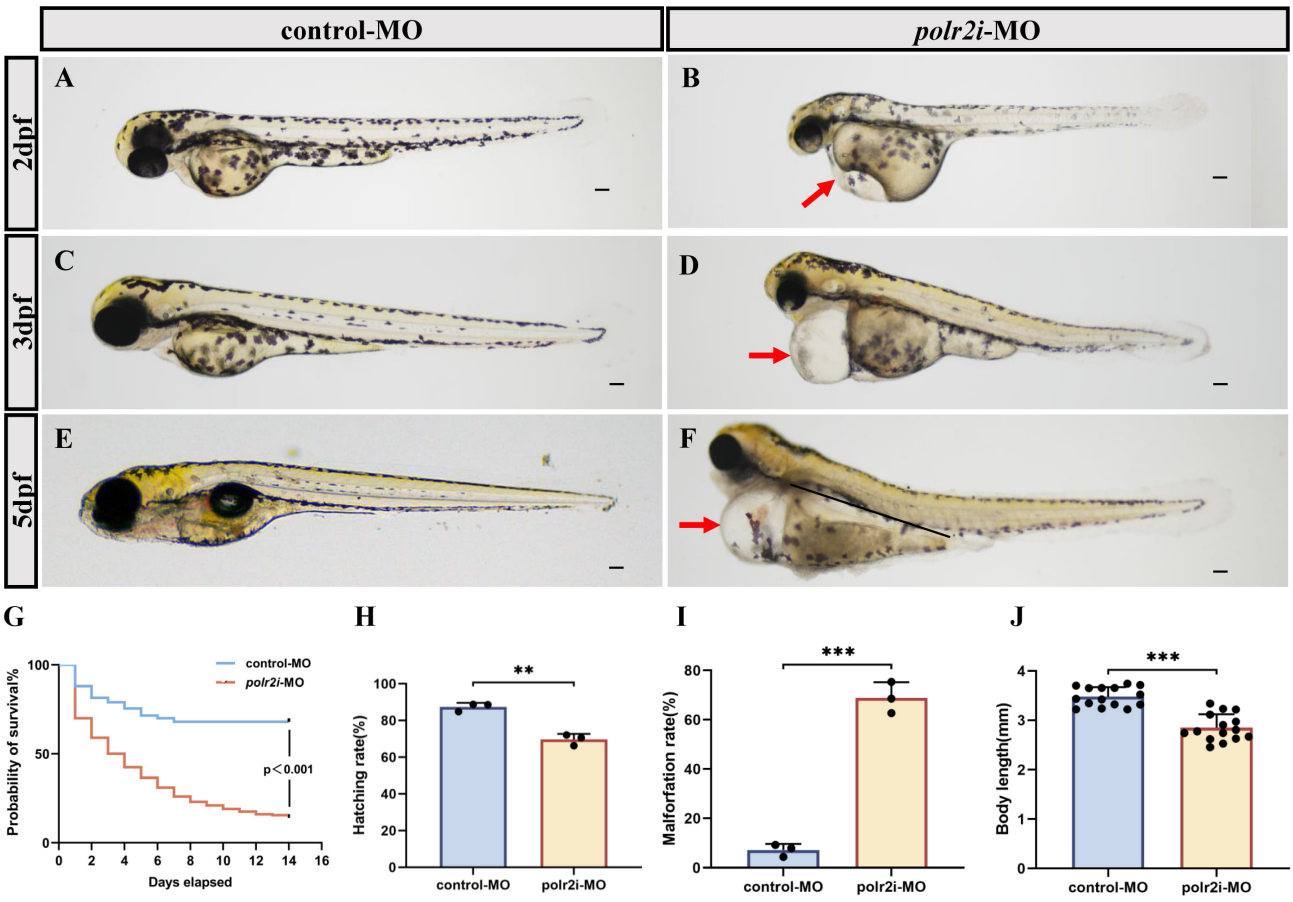

Fig. 2. Aberrant *polr2i* gene function causes developmental defects in zebrafish. (A–F) The bright-field images showed the overall morphology of 2 dpf, 3 dpf and 5 dpf zebrafish embryos injected with control-MO (A,C,E) and *polr2i* gene-MO (B,D,F). (G) Kaplan-Meier plot for control-MO (n = 200) and *polr2i* gene-MO (n = 200) zebrafish embryos. Statistical significance was determined using a log-rank test. The significant *p* value is shown. (H) Hatching rates at 72 hpf (n = 200, N = 3). (I) Malformation rates at 72 hpf (n = 200, N = 3). (J) Body length at 72 hpf (n = 15, N = 3). The red arrows indicate the pericardial edema. The scale bar represents 100 µm. **, $p < 0.01$, ***, $p < 0.001$.

gene mutations in CHD. RT-PCR analysis demonstrated that morpholino-mediated knockdown induced intron retention and exon extension, consistent with a splicing-through mechanism rather than exon skipping (Fig. 1C,D). Effective knockdown of *polr2i* gene was achieved by inhibiting e1i1 linkage leading to a direct read to the intron and confirmed by qRT-PCR (Fig. 1E). This validated knockdown model was utilized in subsequent experiments.

3.2 polr2i Gene Deficiency Impairs Regular Development of Zebrafish

Following standard morpholino administration protocols, we performed dose-response testing through serial dilutions, and it was found that during zebrafish embryo development, the survival rate gradually decreased with the increase of the concentration while the malformation rate increased with the increase of the concentration, and the final concentration was determined to be 4.8 µg/µL, and the injection volume of each embryo was 1 nL, with a total dose of 4.8 ng/embryo (**Supplementary Fig. 1A,B**). *polr2i* gene morphants displayed significantly delayed developmental progression compared to the control group. Conspicuous morphological abnormalities in *polr2i* gene morphants at 2, 3, and 5 days post-fertilization (dpf) included reduced body and eye size, curvature of the body, pericardial edema, and diminished pigmentation (Fig. 2A–F).

To assess the survival of *polr2i* gene morphants, we monitored the survival of control and the *polr2i* gene morphants from the embryonic stage. More than 50% of *polr2i* gene morphants died at 3 days after birth (Fig. 2G). Hatching rate was significantly decreased in the *polr2i* gene morphants compared to the control group (Fig. 2H). In addition, 85% of *polr2i* gene-MO embryos died at 14 dpf. The onset of mortality was frequently preceded by progressive pericardial edema, implicating cardiac dysfunction as a primary factor in the early mortality observed in *polr2i* gene morphants. The rate of malformations increased significantly in the morphant (Fig. 2I) and the body length was signifi-

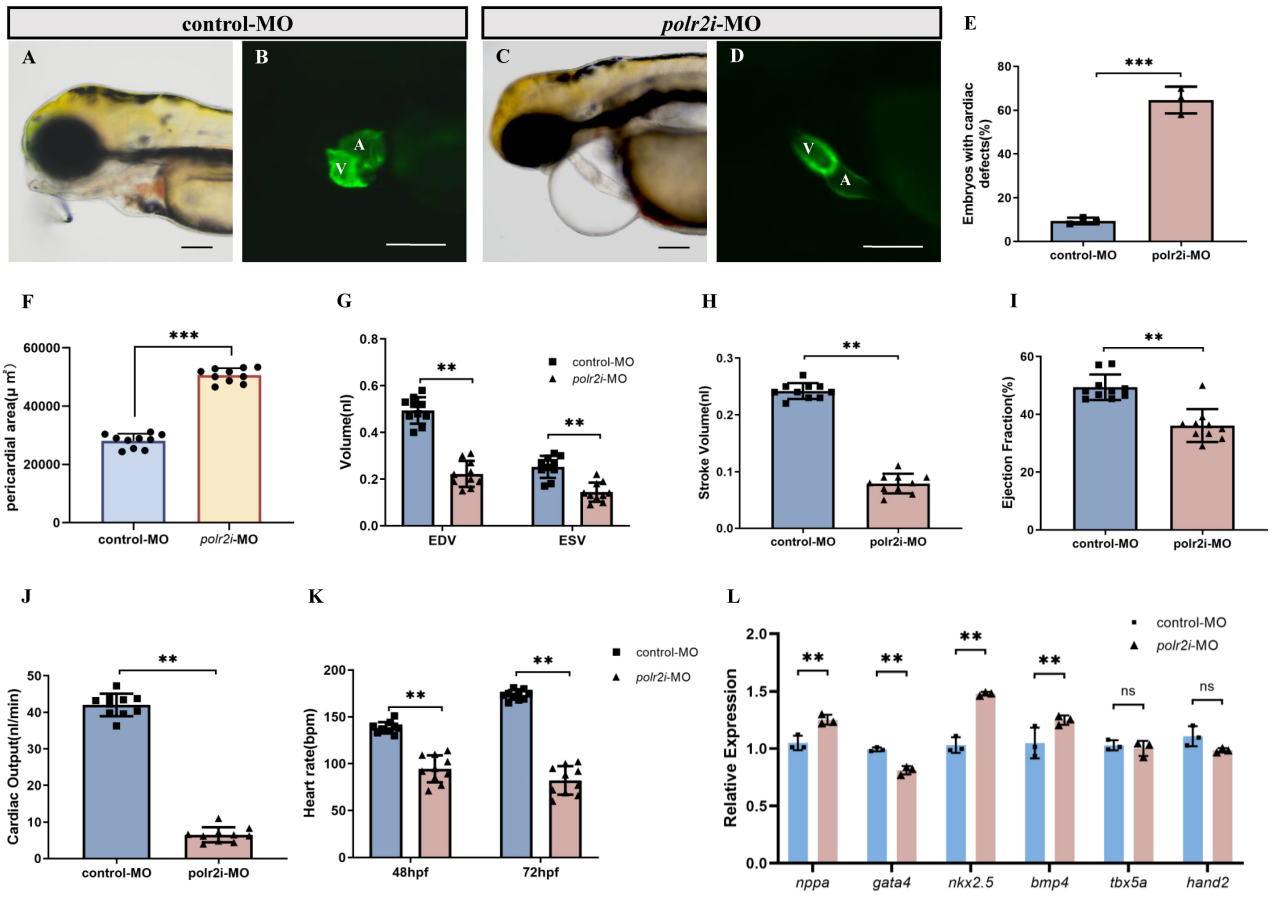

Fig. 3. Effects of *polr2i* gene knockdown on the heart of zebrafish. (A–D) Phenotypes of larvae of *Tg(myl7:EGFP)* lines. (E) Significantly more *polr2i* gene-MO embryos had abnormal cardiac development than control-MO embryos (n = 200, N = 3). (F) Pericardial area at 72 hpf (n = 10, N = 3). (G–K) Quantified analysis data after high-speed photography using ImageJ software. EDV (nL), ESV (nL), stroke volume (nL), ejection fraction, heart rate (per minute) and cardiac output (nL/min) in 72 hpf control-MO (n = 10, N = 3) and *polr2i* gene-MO (n = 10, N = 3) zebrafish embryos. (L) The expression levels of genes related to heart development in zebrafish embryos were detected using qRT-PCR technology after *polr2i*-MO knockdown or control-MO treatment (n = 50, N = 3). The scale bar represents 100 μm. A, atrium; V, ventricle. Student's *t*-test, **, $p < 0.01$, ***, $p < 0.001$, ns: no statistical difference.

cantly decreased in the *polr2i* gene morphants compared to the control group (Fig. 2J).

It is worth noting that when the *polr2i* gene was supplemented, the developmental abnormality related phenotype of zebrafish at 3 dpf was rescued. According to phenotype speculation, there may be a dose effect of mRNA. Using different concentrations of *polr2i* gene-MO:*polr2i* gene-mRNA (1:1; 1:2; 1:3), it was found that there was no significant difference in the phenotype of different concentrations of replenishment injection (**Supplementary Fig. 2A**). Compared with the knockout group, the total mortality rate (**Supplementary Fig. 2B**), malformation rate (**Supplementary Fig. 2C**), heart rate (**Supplementary Fig. 2D**), body length (**Supplementary Fig. 2E**), pericardial area (**Supplementary Fig. 2F**), and eye area (**Supplementary Fig. 2G**) of the supplementation group showed statistical differences, but there were no significant differences within each supplementation group. Overall, these results indicate that *polr2i* gene plays a crucial role in the developmental stages of zebrafish.

3.3 polr2i Gene Knockdown Led to Impaired Cardiac Performance

To assess structural heart abnormalities in *polr2i* gene knockdown embryos, we examined the hearts of 72 hpf embryos injected with control-MO and *polr2i* gene-MO, utilizing the *Tg(myl7:GFP)* transgenic strain that highlights the myocardium in green fluorescent protein (Fig. 3A–D). We observed elongated, string-like heart tubes with minimal overlap between the ventricle and atrium. And in the population of zebrafish larvae with low expression of *polr2i* gene, the incidence of cardiac abnormalities is much higher than that of the control group (Fig. 3E). Notably, by 72 hpf, pericardial edema was significantly exacerbated

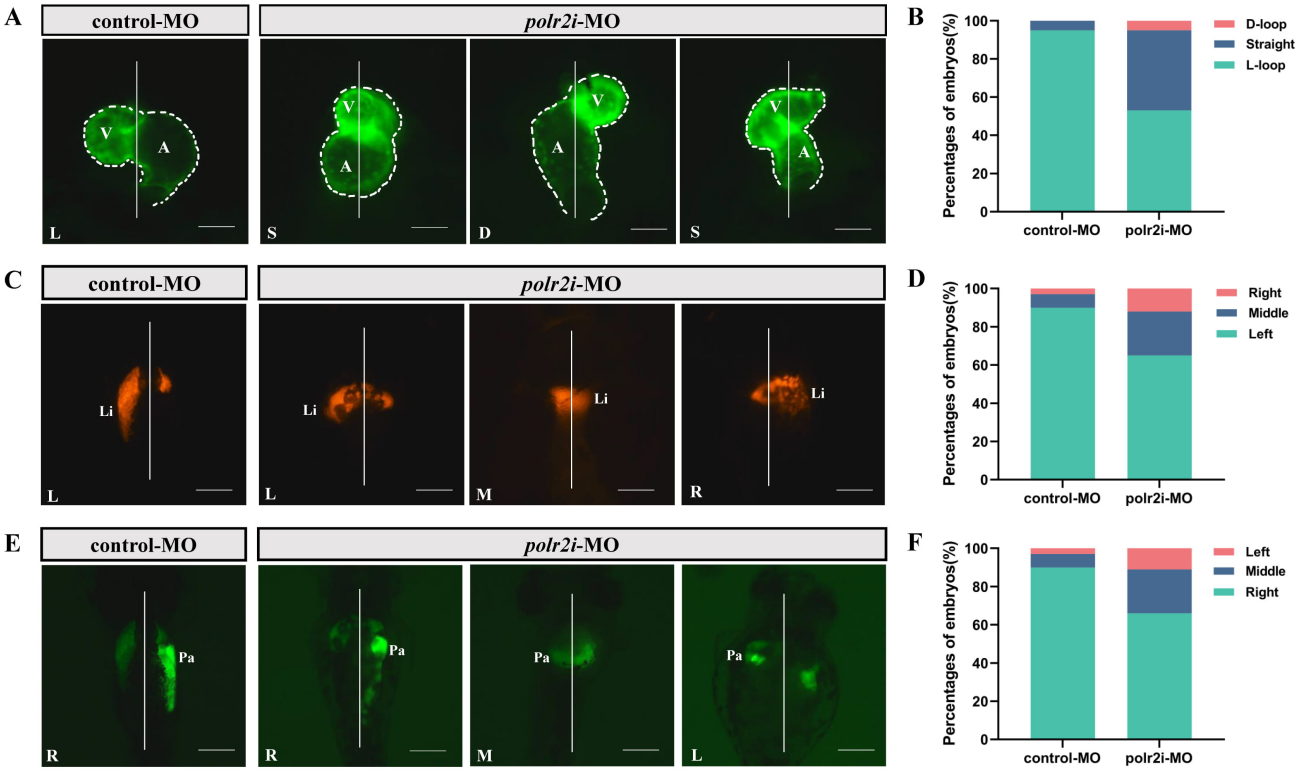

Fig. 4. *polr2i* gene regulates the left-right asymmetry at early stage during zebrafish embryogenesis. (A) Dorsal view of embryonic hearts at 72 hpf in *Tg(myl7:EGFP)* lines (n = 10, N = 3). L, L-loop; S, Straight; D, D-loop. (B) Cardiac phenotype distribution of embryos injected with control-MO or *polr2i* gene-MO (n = 10, N = 3). (C) Dorsal view of embryonic livers at 72 hpf in *Tg(fabp10a:dsRed)* lines (n = 10, N = 3). L, Left; M, Middle; R, Right. (D) Hepatic phenotype distribution of embryos injected with control-MO or *polr2i* gene-MO (n = 10, N = 3). (E) Dorsal view of embryonic pancreas at 72 hpf in *Tg(ela3l:EGFP)* lines (n = 10, N = 3). L, Left; M, Middle; R, Right. (F) Pancreatic phenotype distribution of embryos injected with control-MO or *polr2i* gene-MO (n = 10, N = 3). The scale bar represents 100 µm. A, atrium; V, ventricle; Li, liver; Pa, pancreas.

(Fig. 3F), indicating severe cardiac malformations or functional deficits in *polr2i* gene mutants.

To evaluate *polr2i* gene-MO hearts for functional deficits, we measured ejection fraction and cardiac output in 72 hpf embryos. We used fluorescence microscopy to capture dynamic images of *GFP*+ hearts in control-MO and *polr2i* gene-MO *Tg(myl7:GFP)* transgenic embryos over several cardiac cycles. We extracted dynamic chamber volumes over time, including end-diastolic volume (EDV) and end-systolic volume (ESV). EDV and ESV were significantly reduced in *polr2i* gene morphant embryos (Fig. 3G). Three indices of ventricular function, all of which are calculated from EDV and ESV, were also significantly reduced. These include stroke volume SV = EDV – ESV, ejection fraction EF = SV/EDV and cardiac output (stroke volume × heart rate; Fig. 3H,I,J). The reduced ejection fraction is suggestive of systolic heart failure stemming from compromised cardiomyocyte contraction. In addition to these structural defects, decreased heart rate was also detected in *polr2i* gene morphant embryos at 48 and 72 hpf (Fig. 3K). Reduced ventricular and atrial contractility resulting in slower blood flow compared to control embryos.

Additionally, qRT-PCR analysis at 72 hpf revealed significant alterations in cardiovascular gene expression in *polr2i* gene morphant (Fig. 3L). Expressions of cardiac markers such as *nppa*, *nkx2.5*, and *bmp4* were elevated, whereas *gata4* showed reduced expression in *polr2i* gene-MO embryos, highlighting potential cardiovascular malformations resulting from the loss of *polr2i* gene function.

3.4 polr2i Gene Regulates the Left-Right Asymmetry at Early Stage During Zebrafish Embryogenesis

Vertebrates exhibit distinct left-right asymmetries in the structure and positioning of their cardiovascular and gastrointestinal systems. Abnormalities in these asymmetries lead to a wide range of congenital defects, including heart malformations.

We observed significant disturbances in cardiac left-right asymmetric patterning or looping in about 47% of *polr2i* gene-MO embryos at 72 hpf, including anomalies such as straight and D-looped heart tubes (Fig. 4A,B). Similar laterality abnormalities in the liver and pancreas were also noted in *polr2i* gene mutants compared to controls (Fig. 4C–F), emphasizing the important role of *polr2i* gene

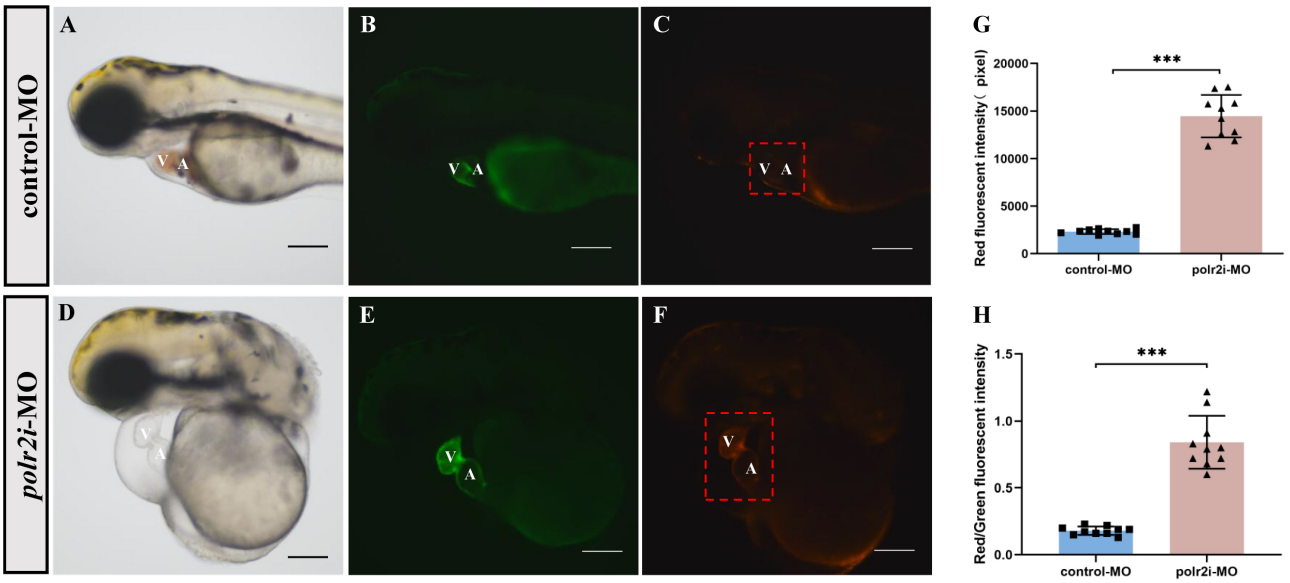

Fig. 5. Morpholino knockdown of *polr2i* gene impairs the myocardial mitochondrial quality in zebrafish. (A–F) The embryos injected with control or *polr2i* gene morpholino were analyzed under light (A,D) and fluorescence microscopy (B,C,E,F) for heart defects at 72 hpf. (G) Red fluorescence intensity of myocardium in *Tg(cmlc2:MitoTimer)* embryos injected with control-MO (n = 10) or *polr2i* gene-MO (n = 10). (H) (Red fluorescence intensity)/(green fluorescence intensity) of myocardium in *Tg(myl7:EGFP;MitoTimer:dsRed)* embryos injected with control-MO (n = 10) or *polr2i* gene-MO (n = 10). The scale bar represents 100 µm. Square: control group; Triangle: experimental group. The red box highlights the heart region. A, atrium; V, ventricle; ***, $p < 0.001$.

in the development of left-right asymmetry in zebrafish. The precise mechanisms underlying these defects require further investigation.

3.5 Knockdown of polr2i Gene Impairs the Myocardial Mitochondrial Quality

Recent studies highlight the critical roles of mitochondrial dynamics and autophagy in cardiac health, emphasizing the balance between mitochondrial biogenesis and mitophagy to maintain mitochondrial number [24]. To evaluate mitochondrial quality and turnover rate, we utilized the MitoTimer—a mutant of the red fluorescent protein where fluorescence transitions from green to red as the protein matures—targeted to the mitochondrial matrix with a mitochondrial-targeting sequence. This construct was introduced into myocardial tissue using Tol2 technology to generate transgenic zebrafish expressing myocardium-specific mitochondrial markers.

We knocked down the *polr2i* gene in *Tg(cmlc2:MitoTimer)* transgenic zebrafish embryos to explore the relationship between *polr2i* gene expression and mitochondrial integrity (Fig. 5A–F). By 72 hpf, fluorescence microscopy revealed a significant reduction in mitochondrial quality and turnover rate in *polr2i* gene knockdown embryos compared to controls (Fig. 5G,H). This suggests that there is a correlation between *polr2i* gene knockdown, myocardial mitochondrial turnover and cardiac development.

3.6 Loss of polr2i Gene Induces Vascular Defects and Poor Blood Flow In Vivo

Cardiac malformations are often associated with vascular abnormalities and compromised blood circulation. In control-MO injected *Tg(fli1a:EGFP)* zebrafish embryos, vascular structures, including natural intersegmental vessels (ISVs), appeared regular by 3 dpf (Fig. 6A,B). Conversely, *polr2i* gene-MO injected embryos exhibited significant angiogenesis impairment, characterized by a reduced number and length of ISVs (Fig. 6C–F). The caudal vein plexus (CVP), typically forming honeycomb-like structures at the tail by 3 dpf in controls, showed fewer loops in *polr2i* gene-MO embryos (Fig. 6B,D,G).

In addition, *polr2i* gene-mutated embryos often exhibit blood accumulation and clotting in the heart chamber and blood vessels. O-anisidine staining showed red blood cells (RBCs) accumulation. Compared with the control group (Fig. 7A–D), it was significantly enhanced in *polr2i* gene knockdown embryos (Fig. 7E–H), especially at 96 hpf, highlighting the serious vascular and circulatory damage caused by *polr2i* gene deletion. Morphometric quantification confirmed 1.8 ± 0.3-fold expansion of congested areas in morphants (Fig. 7I).

4. Discussion

Previous investigations highlighted that *POLR2I* gene might be a potential pathogenic gene for CHD in fetuses. Our comprehensive literature review revealed no existing reports linking POLR2I protein functional deficiencies with

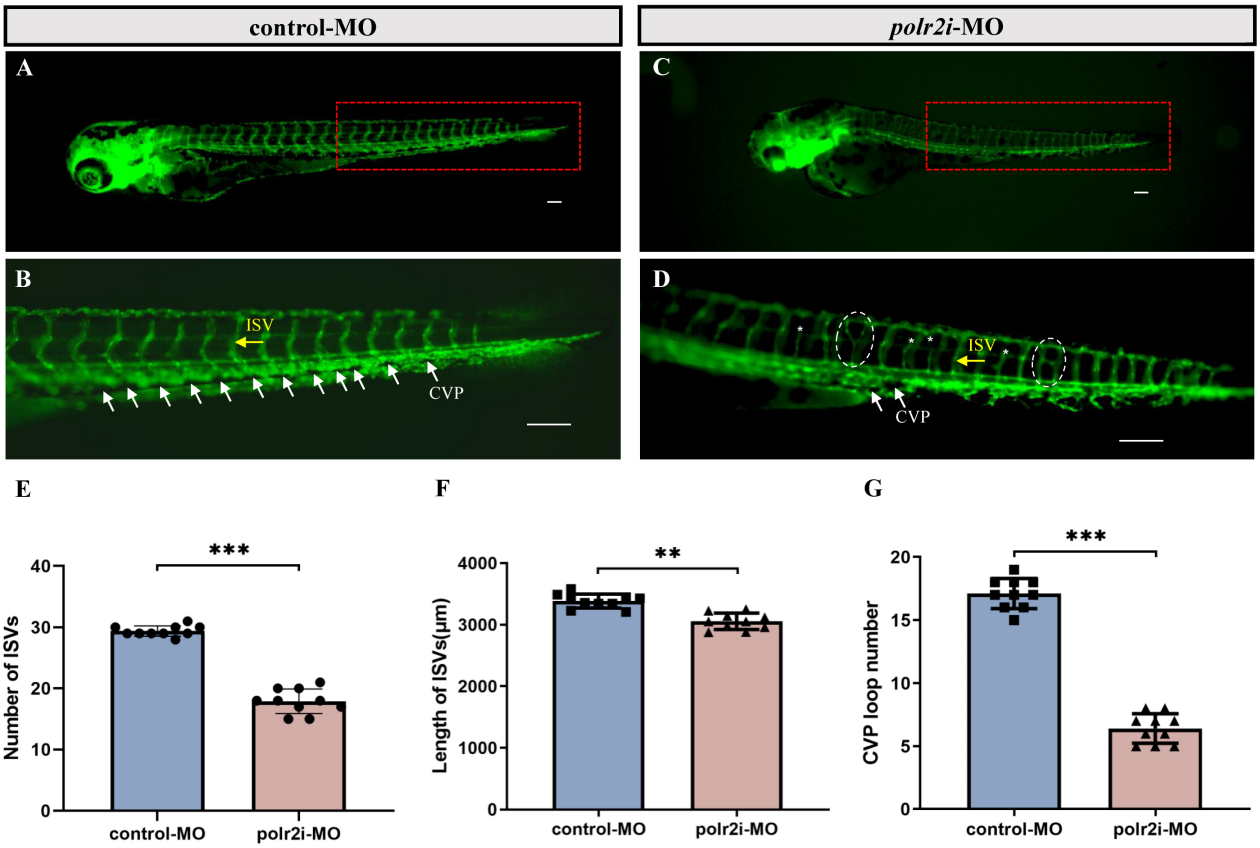

Fig. 6. Morpholino knockdown of *polr2i* gene impairs the angiogenesis and CVP formation in zebrafish. (A–D) Representative fluorescent images of *Tg*(*fli1a:EGFP*) embryos at 72 hpf, with the vascular structures visualized by EGFP fluorescence. The red boxed regions of (A,C) are shown at a higher magnification in (B,D), respectively (Yellow arrow: Internodal blood vessels; White arrow: Tail vein plexus; White dashed box: vascular compensatory hyperplasia phenomenon. n = 10). (B) ISVs and CVP showed regular development in the embryos injected with control-MO (n = 10). (D) Compared with the control group, embryos injected with *polr2i* gene-MO presented a lower number of incomplete ISVs and specific defects in CVP formation (n = 10). (E) Quantification of the number of complete ISVs shows a decrease in *polr2i* gene morphants (n = 10). (F) Quantification of the total length of the ISVs shows a decrease in *polr2i* gene morphants (n = 10). (G) Quantification of loop formation at CVP shows a decrease in *polr2i* gene morphants (n = 10). ISV, intersegmental vessel; CVP, caudal vein plexus. The scale bar represents 100 μm. Square: control group; Triangle: experimental group. **, $p < 0.01$, ***, $p < 0.001$.

CHD, nor were any relevant animal models reported on ZFIN (https://zfin.org/). Our phylogenetic analysis demonstrated that POLR2I protein is conserved across vertebrates, suggesting that the zebrafish could serve as a viable *in vivo* model for studying *polr2i* gene's role in cardiac regulation. Expression analysis via qRT-PCR confirmed that *polr2i* gene is active throughout various developmental stages in zebrafish, underscoring its potential significance in embryogenesis.

This study utilized a gene knockout model to reveal the important function of *polr2i* gene deficiency in zebrafish heart development. However, due to the lack of cell type specificity in current models, it is not possible to specify at least what specific cell damage/death is causing a series of cardiac developmental phenotypes. Based on the cells involved in cardiac development, we boldly speculate that there may be several types of cells: (1) Cardiomyocyte, during cardiac development, the differentiation of cardiomyocytes promotes myocardial proliferation, and the functions of cardiac contraction/relaxation are closely related to cardiomyocytes [25]. (2) Epicardial cells, study has shown that epicardial myocardial crosstalk is necessary for regulating ventricular volume during the early epicardial attachment stage (52–96 hpf) [26]. Epicardial cells are closely related to the formation of the pericardium, which wraps around the myocardium after formation, and secreted factors derived from the epicardium promote the growth of ventricular cardiomyocytes [27]. The current association between POLR2I protein and congenital heart disease (CHD) has not been systematically validated through large-scale prospective cohort studies. The functional evidence provided by the zebrafish model in this study can provide

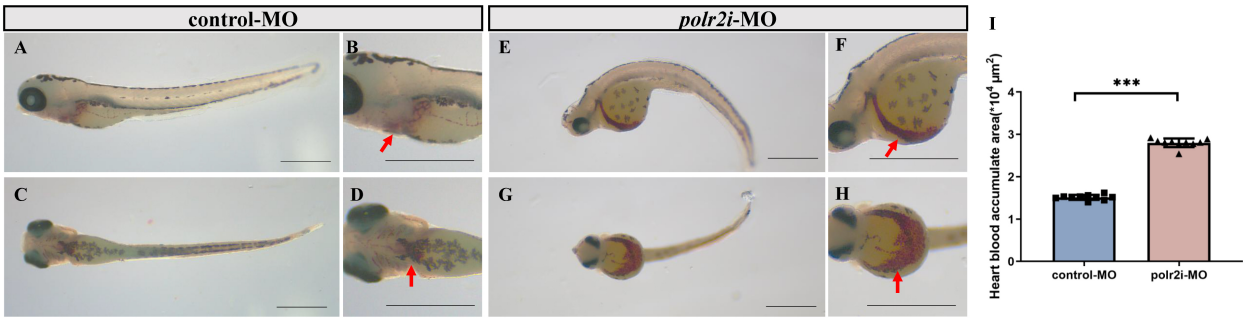

Fig. 7. Morpholino knockdown of *polr2i* gene impairs the blood circulation in zebrafish. (A–D) The staining of hemoglobin in the control-MO group at 96 hpf. (E–H) The staining of hemoglobin in the *polr2i* gene-MO group at 96 hpf. (I) Quantify the areas of their erythrocyte aggregation. The red arrows indicate red blood cells accumulation in heart (n = 10). The scale bar represents 100 μm. Square: control group; Triangle: experimental group. ***, $p < 0.001$.

experimental support for evaluating the pathogenicity of this gene, but its clinical relevance still needs to be further confirmed in combination with human genetic data in the future.

Utilizing Morpholino Mediated Gene Editing, we successfully downregulated *polr2i* gene expression in zebrafish. MO could affect the splicing modification of precursor mRNA, which it was an effective experimental technique. This intervention, verified by qRT-PCR, disrupted normal embryonic development, which was partially rescued by *polr2i* gene-mRNA supplementation, confirming the phenotype's direct association with *polr2i* gene downregulation. Knocking down *polr2i* gene caused developmental malformation phenotypes such as pericardial edema, atrial ventricular linearization, abnormal cardiac cyclization, and impaired cardiac function in zebrafish embryos and it was shown that genes related to cardiac development are affected, suggesting that *polr2i* gene may be involved in early cardiac development in zebrafish. The research team utilized whole zebrafish embryos for RNA extraction due to the impracticality of isolating cardiac tissues from the microscale embryonic heart. Based on whole embryo qRT-PCR analysis, the transcription levels of heart development related genes (nppa, gata4, nkx2.5, bmp4) were altered, suggesting that *polr2i* gene may be involved in the early heart development process of zebrafish. It should be noted that due to the difficulty in separating zebrafish embryonic heart tissue at the microscale, this study used whole embryo RNA extraction, which has clear limitations. This approach contrasts with established findings from prior studies: WISH (Whole-mount *In Situ* Hybridization) analyses have demonstrated cardiac-specific expression patterns of the *gata4* and *nkx2.5* genes [28]. However, there is cardiac expression of *bmp4* at 72 hpf, as well as non-cardiac expression. It is definitely present in fins, cloaca, ear sacs and smooth muscle cells [29–33]. Although Bmp4 is expressed in non-cardiac tissues, its critical role in cardiac development supports phenotypic relevance [34,35]. Meanwhile, we observed impaired formation of ISVs and CVP, as well as stagnation of blood flow in mutant zebrafish, indicating that knocking down *polr2i* gene also affects vascular development and blood circulation processes.

Although this study supports the conclusions through rigorous morpholino generation control experiments, future independent validation in combination with CRISPR/Cas9 knockdown or a second morpholino generation of the target locus will be required according to the current standards for gene function studies in zebrafish [22]. We have started to design gRNAs targeting *polr2i* gene exon 3 and plan to obtain F0 mosaic mutants by microinjection and compare their phenotypic concordance with the morpholino generation phenotype.

The uninterrupted contraction function of heart is closely related to the supply of energy. Cardiomyocytes, as the main working unit of cardiac contraction and pumping, have high energy demand. Mitochondria account for 35% of cardiomyocytes volume, and the ATP produced by mitochondria through oxidative phosphorylation is necessary to maintain cardiomyocytes contraction [36]. Mitochondria plays an important role in the development and physiological function of the heart [37,38]. We utilized the transgenic line *Tg(cmlc2:MitoTimer)*, which expresses the MitoTimer probe specifically in myocardial cells. Timer, the mutant of DsRed fluorescent protein, as a reporter for mitochondrial dynamics, provides clues for mitochondrial functional status with the fluorescence changes from green to red over time [39]. Normally, MitoTimer displays different maturation stages (from green to red) evenly throughout the mitochondrial network. Increased red/green fluorescence ratio implies decreased mitochondrial turnover rate, which can indicate the age and renewal status of mitochondria [40]. In addition, in the previous study, MitoTimer reported that certain genes may be associated with the occurrence of mitochondrial oxidative stress and damage *in vivo* [41]. However, we used MitoTimer to monitor the mitochondrial quality and turnover rate of zebrafish cardiomyocytes [39,42].

The experimental results indicate that low expression of *polr2i* gene would break the homeostasis of mitochondria dynamics, and further destroy the normal cardiac function of zebrafish myocardium.

The process by which a vertebrate embryo develops into a living organism with asymmetrical features, such as anterior-posterior, dorsal-ventral, and left-right, remains a significant challenge in the field of developmental biology [43]. Left-right asymmetry is a common phenomenon in the natural world, and maintaining accurate left-right patterns is essential for proper embryonic development. Disruptions in these patterns can lead to developmental defects [44]. Cells and molecules within the heart field of the anterior lateral plate mesoderm (ALPM) exhibit differences between the left and right sides, indicating that cardiac development is inherently lateralized. As the primitive heart tube forms, this asymmetry persists and becomes more pronounced with the cyclization of the heart tube. Following the formation of the heart chambers and the inflow and outflow regions, the heart's position relative to the midline further emphasizes these left-right differences [45]. Clinical studies and animal experiments have demonstrated that the left-right axis significantly influences heart development. Complex CHD often arise from imbalances in this left-right asymmetrical pattern [46]. In our studies, we utilized transgenic zebrafish with specific fluorescent protein markers for the heart, liver, and pancreas. The knockdown of *polr2i* gene led to malformed heart cyclization and abnormal lateralization of the liver and pancreas, highlighting the crucial role of this gene in maintaining correct developmental patterns.

In conclusion, our findings affirm *polr2i* gene's integral role in zebrafish embryogenesis, particularly in cardiac and mitochondrial function. While this study lays foundational knowledge, further research is required to elucidate the specific mechanisms through which *polr2i* gene influences cardiac development. These insights could propel novel therapeutic strategies for managing CHD, emphasizing the need for continued investigation into this critical gene.

5. Conclusion

The study shows that *polr2i* gene knockdown leads to pathological changes in developing zebrafish. The results indicate that *polr2i* gene is required for early cardiac development in zebrafish, which might contribute to understanding the biological function of the human *POLR2I* gene.

Availability of Data and Materials

The data that support the findings of this study are available from the corresponding author upon reasonable request.

Author Contributions

YKC: Writing — original draft, Writing — review & editing, Methodology, Formal Analysis, Visualization. QPZ: Writing — original draft, Investigation, Methodology, Data curation. XYP: Investigation, Funding acquisition. XRW: Writing — review & editing, Visualization, Supervision. HC: Conceptualization, Writing — review & editing. QC: Resources, Conceptualization, Project administration, Funding acquisition. STH: Resources, Methodology, Funding acquisition; YQL: Writing — review & editing, Conceptualization, Funding acquisition. All authors contributed to editorial changes in the manuscript. All authors read and approved the final manuscript. All authors have participated sufficiently in the work and agreed to be accountable for all aspects of the work.

Ethics Approval and Consent to Participate

All animal procedures of this research were conducted in compliance with ethical standards. This study has been approved by the Animal Ethics Committee of Fujian Maternity and Child Health Hospital (Approval Number: AEC SFY 2025058). This study was arranged in strict accordance with the ARRIVE guidelines.

Acknowledgment

We would like to express our gratitude to all those who helped us during the writing of this manuscript.

Funding

This work was supported by the grants from the Startup Fund for scientific research, Fujian Medical University [grant numbers 2023QH1197]; Youth scientific research project of Fujian Provincial Health Commission [grant numbers 2024QNA059 and 2024QNB004]; The Fujian Provincial Natural Science Foundation of China [grant numbers 2025J011205 and 2025J011206].

Conflict of Interest

The authors declare no conflict of interest.

Supplementary Material

Supplementary material associated with this article can be found, in the online version, at https://doi.org/10.31083/FBL44633.

References

[1] Hinton RB, Ware SM. Heart Failure in Pediatric Patients With Congenital Heart Disease. Circulation Research. 2017; 120: 978–994. https://doi.org/10.1161/CIRCRESAHA.116.308996.

[2] Oh H. Cell Therapy Trials in Congenital Heart Disease. Circulation Research. 2017; 120: 1353–1366. https://doi.org/10.1161/CIRCRESAHA.117.309697.

[3] Andersen TA, Troelsen KDLL, Larsen LA. Of mice and men: molecular genetics of congenital heart disease. Cellular and

Molecular Life Sciences: CMLS. 2014; 71: 1327–1352. https://doi.org/10.1007/s00018-013-1430-1.

[4] Lage K, Greenway SC, Rosenfeld JA, Wakimoto H, Gorham JM, Segrè AV, *et al*. Genetic and environmental risk factors in congenital heart disease functionally converge in protein networks driving heart development. Proceedings of the National Academy of Sciences of the United States of America. 2012; 109: 14035–14040. https://doi.org/10.1073/pnas.1210730109.

[5] Bruneau BG. Signaling and transcriptional networks in heart development and regeneration. Cold Spring Harbor Perspectives in Biology. 2013; 5: a008292. https://doi.org/10.1101/cshperspect.a008292.

[6] Mitchell ME, Sander TL, Klinkner DB, Tomita-Mitchell A. The molecular basis of congenital heart disease. Seminars in Thoracic and Cardiovascular Surgery. 2007; 19: 228–237. https://doi.org/10.1053/j.semtcvs.2007.07.013.

[7] Stephen J, Maddirevula S, Nampoothiri S, Burke JD, Herzog M, Shukla A, *et al*. Bi-allelic TMEM94 Truncating Variants Are Associated with Neurodevelopmental Delay, Congenital Heart Defects, and Distinct Facial Dysmorphism. American Journal of Human Genetics. 2018; 103: 948–967. https://doi.org/10.1016/j.ajhg.2018.11.001.

[8] Deng H, Xia H, Deng S. Genetic basis of human left-right asymmetry disorders. Expert Reviews in Molecular Medicine. 2015; 16: e19. https://doi.org/10.1017/erm.2014.22.

[9] Shiraishi I, Ichikawa H. Human heterotaxy syndrome – from molecular genetics to clinical features, management, and prognosis –. Circulation Journal: Official Journal of the Japanese Circulation Society. 2012; 76: 2066–2075. https://doi.org/10.1253/circj.cj-12-0957.

[10] Tan M, Wang X, Liu H, Peng X, Yang Y, Yu H, *et al*. Genetic Diagnostic Yield and Novel Causal Genes of Congenital Heart Disease. Frontiers in Genetics. 2022; 13: 941364. https://doi.org/10.3389/fgene.2022.941364.

[11] Rémy S, Tesson L, Ménoret S, Usal C, Scharenberg AM, Anegon I. Zinc-finger nucleases: a powerful tool for genetic engineering of animals. Transgenic Research. 2010; 19: 363–371. https://doi.org/10.1007/s11248-009-9323-7.

[12] Acker J, Wintzerith M, Vigneron M, Kedinger C. Structure of the gene encoding the 14.5 kDa subunit of human RNA polymerase II. Nucleic Acids Research. 1993; 21: 5345–5350. https://doi.org/10.1093/nar/21.23.5345.

[13] Hull MW, McKune K, Woychik NA. RNA polymerase II subunit RPB9 is required for accurate start site selection. Genes & Development. 1995; 9: 481–490. https://doi.org/10.1101/gad.9.4.481.

[14] Nesser NK, Peterson DO, Hawley DK. RNA polymerase II subunit Rpb9 is important for transcriptional fidelity in vivo. Proceedings of the National Academy of Sciences of the United States of America. 2006; 103: 3268–3273. https://doi.org/10.1073/pnas.0511330103.

[15] Berkyurek AC, Furlan G, Lampersberger L, Beltran T, Weick EM, Nischwitz E, *et al*. The RNA polymerase II subunit RPB-9 recruits the integrator complex to terminate Caenorhabditis elegans piRNA transcription. The EMBO Journal. 2021; 40: e105565. https://doi.org/10.15252/embj.2020105565.

[16] McKune K, Moore PA, Hull MW, Woychik NA. Six human RNA polymerase subunits functionally substitute for their yeast counterparts. Molecular and Cellular Biology. 1995; 15: 6895–6900. https://doi.org/10.1128/MCB.15.12.6895.

[17] Harrison DA, Mortin MA, Corces VG. The RNA polymerase II 15-kilodalton subunit is essential for viability in Drosophila melanogaster. Molecular and Cellular Biology. 1992; 12: 928–935. https://doi.org/10.1128/mcb.12.3.928-935.1992.

[18] Talukdar HA, Foroughi Asl H, Jain RK, Ermel R, Ruusalepp A, Franzén O, *et al*. Cross-Tissue Regulatory Gene Networks in Coronary Artery Disease. Cell Systems. 2016; 2: 196–208. https://doi.org/10.1016/j.cels.2016.02.002.

[19] You S, Xu J, Wu B, Wu S, Zhang Y, Sun Y, *et al*. Comprehensive Bioinformatics Analysis Identifies *POLR2I* as a Key Gene in the Pathogenesis of Hypertensive Nephropathy. Frontiers in Genetics. 2021; 12: 698570. https://doi.org/10.3389/fgene.2021.698570.

[20] Brown DR, Samsa LA, Qian L, Liu J. Advances in the Study of Heart Development and Disease Using Zebrafish. Journal of Cardiovascular Development and Disease. 2016; 3: 13. https://doi.org/10.3390/jcdd3020013.

[21] Matrone G, Wilson KS, Mullins JJ, Tucker CS, Denvir MA. Temporal cohesion of the structural, functional and molecular characteristics of the developing zebrafish heart. Differentiation; Research in Biological Diversity. 2015; 89: 117–127. https://doi.org/10.1016/j.diff.2015.05.001.

[22] Stainier DYR, Raz E, Lawson ND, Ekker SC, Burdine RD, Eisen JS, *et al*. Guidelines for morpholino use in zebrafish. PLoS Genetics. 2017; 13: e1007000. https://doi.org/10.1371/journal.pgen.1007000.

[23] Matthews M, Varga ZM. Anesthesia and euthanasia in zebrafish. ILAR Journal. 2012; 53: 192–204. https://doi.org/10.1093/ilar.53.2.192.

[24] Ikeda Y, Sciarretta S, Nagarajan N, Rubattu S, Volpe M, Frati G, *et al*. New insights into the role of mitochondrial dynamics and autophagy during oxidative stress and aging in the heart. Oxidative Medicine and Cellular Longevity. 2014; 2014: 210934. https://doi.org/10.1155/2014/210934.

[25] Staudt D, Stainier D. Uncovering the molecular and cellular mechanisms of heart development using the zebrafish. Annual Review of Genetics. 2012; 46: 397–418. https://doi.org/10.1146/annurev-genet-110711-155646.

[26] Boezio GLM, Zhao S, Gollin J, Priya R, Mansingh S, Guenther S, *et al*. The developing epicardium regulates cardiac chamber morphogenesis by promoting cardiomyocyte growth. Disease Models & Mechanisms. 2023; 16: dmm049571. https://doi.org/10.1242/dmm.049571.

[27] Moran HR, Nyarko OO, O'Rourke R, Ching RC, Riemslagh FW, Peña B, *et al*. The pericardium forms as a distinct structure during heart formation. bioRxiv. 2024. https://doi.org/10.1101/2024.09.18.613484. (preprint)

[28] Li S, Li X, Zhao R, Jiang T, Ou Q, Huang H, *et al*. Esketamine induces embryonic and cardiac malformation through regulating the nkx2.5 and gata4 in zebrafish. Scientific Reports. 2025; 15: 7187. https://doi.org/10.1038/s41598-025-91315-2.

[29] Bhakta M, Padanad MS, Harris JP, Lubczyk C, Amatruda JF, Munshi NV. pouC Regulates Expression of bmp4 During Atrioventricular Canal Formation in Zebrafish. Developmental Dynamics: an Official Publication of the American Association of Anatomists. 2019; 248: 173–188. https://doi.org/10.1002/dvdy.2.

[30] Hadzhiev Y, Lele Z, Schindler S, Wilson SW, Ahlberg P, Strähle U, *et al*. Hedgehog signaling patterns the outgrowth of unpaired skeletal appendages in zebrafish. BMC Developmental Biology. 2007; 7: 75. https://doi.org/10.1186/1471-213X-7-75.

[31] Parkin CA, Allen CE, Ingham PW. Hedgehog signalling is required for cloacal development in the zebrafish embryo. The International Journal of Developmental Biology. 2009; 53: 45–57. https://doi.org/10.1387/ijdb.082669cp.

[32] Rothschild SC, Easley CA, 4th, Francescatto L, Lister JA, Garrity DM, Tombes RM. Tbx5-mediated expression of Ca(2+)/calmodulin-dependent protein kinase II is necessary for zebrafish cardiac and pectoral fin morphogenesis. Developmental Biology. 2009; 330: 175–184. https://doi.org/10.1016/j.ydbio.2009.03.024.

[33] Pittlik S, Domingues S, Meyer A, Begemann G. Expression of

zebrafish aldh1a3 (raldh3) and absence of aldh1a1 in teleosts. Gene Expression Patterns: GEP. 2008; 8: 141–147. https://doi.org/10.1016/j.gep.2007.11.003.

[34] Chen JN, van Eeden FJ, Warren KS, Chin A, Nüsslein-Volhard C, Haffter P, *et al*. Left-right pattern of cardiac BMP4 may drive asymmetry of the heart in zebrafish. Development (Cambridge, England). 1997; 124: 4373–4382. https://doi.org/10.1242/dev.124.21.4373.

[35] Wang Z, Liu XY, Yang CX, Zhou HM, Li YJ, Qiu XB, *et al*. Discovery and functional investigation of *BMP4* as a new causative gene for human congenital heart disease. American Journal of Translational Research. 2024; 16: 2034–2048. https://doi.org/10.62347/DGCD4269.

[36] Picca A, Mankowski RT, Burman JL, Donisi L, Kim JS, Marzetti E, *et al*. Mitochondrial quality control mechanisms as molecular targets in cardiac ageing. Nature Reviews. Cardiology. 2018; 15: 543–554. https://doi.org/10.1038/s41569-018-0059-z.

[37] Gao F, Liang T, Lu YW, Fu X, Dong X, Pu L, *et al*. A defect in mitochondrial protein translation influences mitonuclear communication in the heart. Nature Communications. 2023; 14: 1595. https://doi.org/10.1038/s41467-023-37291-5.

[38] Vega RB, Kelly DP. Cardiac nuclear receptors: architects of mitochondrial structure and function. The Journal of Clinical Investigation. 2017; 127: 1155–1164. https://doi.org/10.1172/JCI88888.

[39] Hernandez G, Thornton C, Stotland A, Lui D, Sin J, Ramil J, *et al*. MitoTimer: a novel tool for monitoring mitochondrial turnover. Autophagy. 2013; 9: 1852–1861. https://doi.org/10.4161/auto.26501.

[40] Gottlieb RA, Stotland A. MitoTimer: a novel protein for monitoring mitochondrial turnover in the heart. Journal of Molecular Medicine (Berlin, Germany). 2015; 93: 271–278. https://doi.org/10.1007/s00109-014-1230-6.

[41] Laker RC, Xu P, Ryall KA, Sujkowski A, Kenwood BM, Chain KH, *et al*. A novel MitoTimer reporter gene for mitochondrial content, structure, stress, and damage in vivo. The Journal of Biological Chemistry. 2014; 289: 12005–12015. https://doi.org/10.1074/jbc.M113.530527.

[42] Trudeau KM, Gottlieb RA, Shirihai OS. Measurement of mitochondrial turnover and life cycle using MitoTimer. Methods in Enzymology. 2014; 547: 21–38. https://doi.org/10.1016/B978-0-12-801415-8.00002-3.

[43] Raya A, Izpisúa Belmonte JC. Left-right asymmetry in the vertebrate embryo: from early information to higher-level integration. Nature Reviews. Genetics. 2006; 7: 283–293. https://doi.org/10.1038/nrg1830.

[44] Nakamura T, Hamada H. Left-right patterning: conserved and divergent mechanisms. Development (Cambridge, England). 2012; 139: 3257–3262. https://doi.org/10.1242/dev.061606.

[45] Forrest K, Barricella AC, Pohar SA, Hinman AM, Amack JD. Understanding laterality disorders and the left-right organizer: Insights from zebrafish. Frontiers in Cell and Developmental Biology. 2022; 10: 1035513. https://doi.org/10.3389/fcell.2022.1035513.

[46] Maclean K, Dunwoodie SL. Breaking symmetry: a clinical overview of left-right patterning. Clinical Genetics. 2004; 65: 441–457. https://doi.org/10.1111/j.0009-9163.2004.00258.x.